

Investigation of the collective properties of a degenerate electron gas in aluminum by the (e, 2e) method

N. M. Persiantseva, N. A. Krasil'nikova, and V. G. Neudachin

Nuclear Physics Research Institute of the Moscow State University
(Submitted 20 July 1978)
Zh. Eksp. Teor. Fiz. 76, 1047-1057 (March 1979)

The behavior of the differential cross section of the (e, 2e) reaction in the knockout of electrons from metallic targets by fast electrons is investigated theoretically and experimentally. It is shown that the (e, 2e) method permits the study of the momentum distribution of the target electron prior to the interaction as well as of the collective response of the electron gas to hole formation. Using aluminum films of ~200 Å thickness, coincidence spectra of the final electrons were obtained with energy resolution ΔE = 16 eV in the interval 45° ≤ θ ≤ 51°. The measured angular-correlation functions turned out to be in the main somewhat broader than the dependences of the differential cross sections of the (e, 2e) reaction on q, calculated by using Hartree-Fock wave functions for the isolated atoms. A state called plasmaron, which is characterized by an anomalously narrow momentum distribution, is separated.

PACS numbers: 34.50.He

The momentum distribution of electrons in metals is investigated by the methods of Compton profiles and positron annihilation. These, however, yield information that is averaged over many energy state. The method of (e, 2e) quasielastic knockout of electrons by fast electrons, combined with angular and energy analysis of the spreading particles and their registration for coincidence, makes possible the study of the momentum distribution of electrons that are in a fixed energy state.¹ This permits reliable identification of plasmon satellites of various hole states. Since the plasmon momentum is small, the satellite momentum distribution has practically the same form as the "initial" hole state.

Some of the preliminary results of this study were reported in Refs. 2 and 3.

1. THEORETICAL DESCRIPTION OF THE PROCESS

The cross section for the quasielastic knockout of an electron by an electron (e, 2e) from an atom or a molecule is given, as is well known by the formula¹ (we put ħ = 1)

$$\frac{d^4\sigma}{d\Omega_1 d\Omega_2 dE_1 dE_2} = \frac{m p_1 p_2}{2p' \cos \vartheta_1} \left(\frac{d\sigma}{d\Omega_1} \right)_{\text{lab}}^{fr} \times \sum_{\alpha, f} S_{\alpha, f}^2 |\varphi_{\alpha}(\mathbf{q})|^2 \delta(E_0 - E_1 - E_2 + \varepsilon_0 + \varepsilon_{\alpha, f}) \delta_{\mathbf{q} + \mathbf{p}_0, \mathbf{p}_1 + \mathbf{p}_2} \quad (1)$$

Here dΩ₁ and dΩ₂ are the solid-angle elements that characterize the emission directions of both final electrons, p₁ and p₂ are their momenta, 2p' = p₁ - p₂, E₁ and E₂ are their energies, m is the electron mass, (dσ/dΩ₁)_{lab}^{fr} is the cross section for free scattering of an electron from the incident beam with energy E₀ by an immobile electron through an angle ϑ₁. Next, -q = p₀ - p₁ - p₂ is the recoil momentum, and the quantity

$$|F_{\alpha, f}(\mathbf{q})|^2 = S_{\alpha, f}^2 |\varphi_{\alpha}(\mathbf{q})|^2 \quad (2)$$

is called the form factor of the knocked-out electron, where S_{α, f}² is the spectroscopic factor and is proportional to the square of the corresponding fractional-parentage coefficient,¹ and finally φ_α(q) is the wave function, normalized to unity, of the single-particle state α from

which the electron is knocked out, in the momentum representation. For the simplest atomic cases α = n and α = l.

Given an initial state |0⟩ and given an index α, several final states |α, f⟩ are possible, having different excitation energies ε_{α, f}. The electron initial-state binding energy corresponding to the state |α, f⟩ of the final ions will be designated ε₀ + ε_{α, f} (we find it convenient to regard these quantities as negative).

The form factor is defined by the expression

$$F_{\alpha, f}(\mathbf{q}) = \left(\frac{N}{(2\pi)^3} \right)^{1/2} \int \Psi_{\alpha, f}^*(1, 2, \dots, N-1) e^{-i\mathbf{q}\cdot\mathbf{r}_N} \times \Psi_{\alpha}(1, 2, \dots, N) d\tau_1 d\tau_2 \dots d\tau_N \quad (3)$$

We transform formulas (1)–(3) to accommodate a degenerate electron gas in a metal. We consider two situations typical of such systems.

The first is the knockout of an electron from the conduction band in a metal. Assuming the system to be translationally invariant and employing, as is customary, a plane-wave basis, i.e., α ≡ k, we get from (3)

$$|F_{\alpha, f}(\mathbf{q})|^2 = C_{\alpha}^2 |b_{\mathbf{k}, \alpha, f}|^2 \frac{V}{(2\pi)^3} \delta_{\mathbf{k}, \mathbf{q}} \quad (4)$$

since

$$|\varphi_{\mathbf{k}}(\mathbf{q})|^2 = \frac{V}{(2\pi)^3} \delta_{\mathbf{q}, \mathbf{k}} = \delta(\mathbf{q} - \mathbf{k}) \quad (5)$$

Here b_q is the operation of annihilation of an electron with momentum q, V is the volume of the system, and the factor C = 2^{1/2} reflects the spin degeneracy. Introducing the spectral density⁴

$$A(\mathbf{k}, \varepsilon) = \sum_f |b_{\mathbf{k}, \alpha, f}|^2 \delta(\varepsilon - \varepsilon_f) \quad (6)$$

we rewrite (1) in the form

$$\frac{d^4\sigma}{d\Omega_1 d\Omega_2 dE_1 dE_2} = \frac{m p_1 p_2}{2p' \cos \vartheta_1} \left(\frac{d\sigma}{d\Omega_1} \right)_{\text{lab}}^{fr} C_{\alpha}^2 A(\mathbf{q}, \varepsilon) \delta(\mathbf{q} + \mathbf{p}_0 - \mathbf{p}_1 - \mathbf{p}_2) \quad (7)$$

where ε = E₁ + E₂ - E₀ - ε₀.

Expressions (4)–(7) show that the spectral density $A(\mathbf{q}, \varepsilon)$ assumes the role of the form factor for a hole state with energy ε . In particular, the quantity

$$n(\mathbf{q}) = \int_{-\infty}^{\infty} A(\mathbf{q}, \varepsilon) d\varepsilon \quad (8)$$

is well known⁴ to be the summary momentum distribution of electron. The deviation of this quantity from a set function characterizes the deviation of the electron gas from an ideal one. This quantity has been well investigated in experiments on positron annihilation,⁵ but formula (7) shows that the $(e, 2e)$ method provides much more detailed information, and makes it possible to investigate the entire “topology” of the \mathbf{q} and ε dependences directly for the quantity $A(\mathbf{q}, \varepsilon)$ and the collective effects connected with it. Namely, in the case of an ideal Fermi gas the spectral density $A(\mathbf{q}, \varepsilon)$, as a function of ε at fixed \mathbf{q} , is equal to zero everywhere except for a peak of unity intensity located at $\varepsilon = -(k_F^2 - q^2)/2m^*$. For a real electron gas, say in aluminum ($\gamma_s = 2$), calculation in the random phase approximation shows⁶ that at the bottom of the conduction band, say at $q = 0.2k_F$, the quantity $A(\mathbf{q}, \varepsilon)$ as a function of energy has two comparable peaks, one with intensity ~ 0.6 approximately where the single peak is located for an ideal gas, and another (“plasmaron”) with intensity ~ 0.3 at an energy $2\hbar\omega_{p1}$ lower than the bottom of the conduction band ($\hbar\omega_{p1} \approx 15.8$ eV for Al). Thus, this interesting detail can be observed at a rather moderate instrumental resolution $\Delta E \approx 10 - 15$ eV.

An expression equivalent to (7) is well known in nuclear physics,⁷ but has not been widely used there so far [the $(p, 2p)$ reaction is used mainly to investigate relatively light nuclei with few particles, $A \leq 40$, where it is convenient to use the wave functions directly].

The second typical situation which we shall consider is the knockout of an electron from a filled shell [“deep (infinite) hole”]. What is of interest here is the possibility of investigating the collective response of a system of conduction electrons to a sudden appearance of deep hole.⁸ Of importance to us are two simplifying circumstances. First, a deep hole “does not multiply” and its possession of a recoil momentum is immaterial, since the hole is connected with an “infinitely heavy” ion. Second, the collective-excitation momentum is small in comparison with the average value of q . Therefore the form factor of the deep hole α factors out, expression (2) takes the form

$$F_{\alpha, l}(\mathbf{q}) = C_{\alpha} (b_{\alpha})_{\alpha, l} \Psi_{\alpha}(\mathbf{q}), \quad (9)$$

and the formula for the cross section of the process can be written as

$$\frac{d^2\sigma}{d\Omega_1 d\Omega_2 dE_1 dE_2} = \frac{m p_1 p_2}{2p^l \cos \theta_1} \left(\frac{d\sigma}{d\Omega_1} \right)_{\text{lab}}^{\text{fr}} S_{\alpha}^2 Z_{\alpha}(\varepsilon) \times |\varphi_{n_l}(\mathbf{q})|^2 \delta_{\mathbf{q}+\mathbf{p}_0, \mathbf{p}_1+\mathbf{p}_2}. \quad (10)$$

Here $Z_{\alpha}(\varepsilon)$ is the spectral density of the deep hole⁸

$$Z_{\alpha}(\varepsilon) = \sum_l |(b_{\alpha})_{\alpha, l}|^2 \delta(\varepsilon - \varepsilon_l), \quad (11)$$

with the summation carried out over the excited states of the conduction-electron system. Next, $S^2 - 2(2l+1)$ is the spectroscopic factor of the deep hole,¹ $\varphi_{n_l}(\mathbf{q})$ is the

radial part of the wave function of the deep hole in the q -representation.

If the possibility of excitation of plasmon satellites⁹ is taken into account in the Mahan–Nozieres theory,⁸ then the expression for $Z_{\alpha}(\varepsilon)$ becomes^{7, 8, 10}

$$Z_{\alpha}(\varepsilon) = \frac{V_0 e^{-\alpha}}{\Gamma(1-\gamma)} \sum_{n=0}^{\infty} \frac{a^n}{n!} \left(\frac{\xi_0}{\varepsilon - \varepsilon_0 + n\omega_{p1}} \right)^{1-\gamma} \theta(\varepsilon - \varepsilon_0 + \hbar\omega_{p1}), \quad (12)$$

$$\gamma = 2 \sum_{\lambda=0}^{\infty} (2\lambda+1) (\delta_{\lambda}/\pi)^2, \quad a = \omega_{p1}^{-1} \sum_{\mathbf{q}}' |V_{\mathbf{q}}|^2 \frac{q^2}{8\pi e^2} \approx e^2 q_e / \pi \omega_{p1}$$

(a is close to $r_s/6$), the prime denotes that the summation is confined to the region $q < q_c$, where $q \leq \omega_{p1}/v_F$. The remaining symbols are the same as in Refs. 8.

It is easy to add to the resultant picture the volume and surface plasmons due to the passage of a charged particle through a film.^{11, 12}

The indicated complications, however, do not affect the “plasmonless” maximum with $n=0$ in formula (12) or the possibility of investigating its form. We can have here an interesting situation² wherein the cross section of the $(e, 2e)$ process has a threshold singularity, while the x-ray photon absorption (the actual subject of Refs. 8 and 9) is on the contrary suppressed at the threshold, since another physical quantity is involved, the convolution of the function $Z_{\alpha}(\varepsilon)$ with the Green’s function of the conduction electrons for the problem with a nonstationary potential of the deep hole.

When the various broadening factors¹² are taken into account, maxima of finite height, with width on the order of several electron volts, should be observed in fact rather than the singularities corresponding to formula (12). According to (12), however, these maxima should be asymmetrical, and this fact constitutes the second interesting aspect, which calls, however, for an experiment with a resolution $\Delta E \approx 0.2 - 0.4$ eV.

2. DESCRIPTION OF EXPERIMENT

The processes described by formulas (7) and (19) were experimentally investigated with a modified variant of the setup described for the most part in Ref. 14. The measurements were made in a complanar symmetrical geometry, i.e., for a situation wherein \mathbf{p}_0 , \mathbf{p}_1 , and \mathbf{p}_2 lie in one plane, while the energies E_1 and E_2 are equal, as are also the divergence angles of the final electrons ϑ_1 and ϑ_2 . The system for the analysis and registration of the diverging particles consisted of two identical channels that incorporated movable hemispherical electrostatic analyzers having second-order focusing; the radii of the inner and outer spheres were $R_1 = 97$ mm and $R_2 = 103$ mm. The electron detectors were VÉU-6 secondary-emission channel multipliers with multiplication factor $10^7 - 10^8$. The pulses from the multipliers were fed to broadband amplifiers that triggered a coincidence circuit. The resolution time of the coincidence circuit was $\tau = 20$ nsec. A PP-9 scaler was used to count the pulses in the coincidence regime as well as when the electrons were registered in one channel.

The primary electron beam of ~ 10 keV energy was shaped by a three-electrode long-focus gun with a V-

shaped directly heated cathode, with a spherical control electrode, and with a spherical anode. The energy resolution $\Delta E = 10 - 15$ eV corresponds to a relative accuracy $\Delta E/E = (1 - 1.5) \times 10^{-3}$. The voltage sources used to feed the electron gun or to produce the fields in the analyzers and lenses, as well as to feed the VEÜ-6 multipliers, were stabilized within 8×10^{-5} , and the ripple did not exceed 5×10^{-5} . Control and measurement of all the applied voltages was by means of an R345 high-resistance dc potentiometer with accuracy 10^{-5} . The measured voltages were picked off high-resistance dividers made up of wire-wound microresistors.

The resolution attained up to now in $(e, 2e)$ experiments with solid targets was $\Delta E = 130 - 140$ eV.¹⁴⁻¹⁶ To improve the energy resolution with minimum loss of intensity of the registered signal, we decelerated the electrons prior to the analysis of the energy distribution of the spreading particles. This deceleration was produced by immersion cylindrical lenses in whose electric field the energy was decreased by approximately one order of magnitude. The employed lenses consisted of two coaxial cylinders displaced relative to each other along the axis with a ratio $R_{\text{out}}/R_{\text{in}} = 2.5$ ($R_{\text{out}} = 20$ mm), and with exit and entrance diaphragms of 3.5 mm diameter. The outer cylinder was grounded and the inner was under the decelerating potential; its exit diaphragm served simultaneously as the entrance diaphragm of the analyzer. The decelerating lenses collimated the beam of the particles registered in each channel, so that the angular resolution was $\Delta \vartheta_{1/2} = 1^\circ$. The relative placement of the lens and analyzer was such that the beam of decelerated electrons was focused on the entrance to the analyzer. The focal length of the lenses remained practically constant when the incident-electron energy changed by +100 eV at a level $E_0 = 5$ keV. This was important in our case, since the energy dependences of the differential cross section of the $(e, 2e)$ reactions were plotted by varying the primary-beam energy at fixed values of the decelerating and analyzing fields. The constancy of the energy of the registered electrons ensured in turn constancy of the instrumental characteristics of the installation during the entire measurement cycle. The exit diaphragms of the analyzers were also at the decelerating potential. The analyzing voltages on the plates of the spectrometer, $U_{1,2}$, were symmetrical relative to the decelerating voltage. Thus the electrons having an energy

$$E = \frac{e\Delta U}{2} \frac{R_{\text{av}}}{R_2 - R_1},$$

where $\Delta U = U_2 - U_1$ and $R_{\text{av}} = (R_1 + R_2)/2$, satisfying the condition for the passage along the central trajectory of the analyzer, moved along the central equipotential deflecting-field equipotential line whose potential was equal to the potential of the entrance and exit diaphragms. Under this condition, the distortions due to edge effects were minimal. A negative potential close in value to the decelerating one was applied to the inputs of the VEÜ-6 multiplier. As a result, the electrons leaving the analyzer moved in a practically zero field right up to the entry into the detector. The second end of the multiplier was at near-ground potential.

The described procedure yielded the coincidence spec-

tra of the electrons in the $(e, 2e)$ reaction on a solid target in a symmetrical coplanar geometry with an energy resolution $\Delta E = \pm 8$ eV at $E_0 = 10$ keV. The half-width of the spectrum registered in each channel was $\Delta E_{1/2} = 11$ eV.

The targets were self-supporting aluminum films 150–200 Å thick produced by sputtering on a soluble sublayer by a technology described in detail in Ref. 17. The duration of each sputtering was 2–3 sec. The carbon impurity accompanying the sputtering of ultrathin single-crystal films should make a negligible contribution in our case, since the sputtering time of the single-crystal films was at least 20 times longer than the sputtering exposures used by us. It is known that aluminum is easily oxidized not only at atmospheric pressure but also in a vacuum at $p = 10^{-6} - 10^{-5}$ Torr,⁵ and the thickness of the oxidized layer is $\sim 40 - 50$ Å. We have therefore regarded our targets as a two-component system Al + Al₂O₃ with a ratio $\sim 1 : 1$. A batch of finished films was mounted in 18 sockets of a rotating drum, so that the targets could be replaced without breaking the vacuum.

The experiments were performed at a residual gas pressure $p = (2 - 4) \times 10^{-6}$ Torr in the chamber. The vacuum was produced by the Era-250 oil-free vacuum unit. Measurements in the coincidence-counting regime were made at a primary electron beam current $I_0 = 6 \times 10^{-8}$ A. The diameter of the irradiated zone on the target was 2 mm.

3. RESULTS AND DISCUSSION

Figure 1 shows the energy dependence of the differential cross section we obtained for the $(e, 2e)$ process at $\vartheta = 45^\circ$. Each peak on this spectrum represents a definite energy state of the target electrons. Similar spectra, the form of which can be reconstructed from the results shown in Fig. 3 below, were obtained for values $45^\circ \leq \vartheta \leq 51^\circ$, corresponding to values of q , in the direction opposite to that of the primary beam, from 0 to 3 atomic units. The connection between the angle and target-electron momentum q , which follows from the energy and momentum conservation laws for the investigated process, takes in the symmetric coplanar case the form

$$\hbar q = (2mE_1)^{1/2} [2 \cos \theta + (2 + e/E_1)^{1/2}]. \quad (13)$$

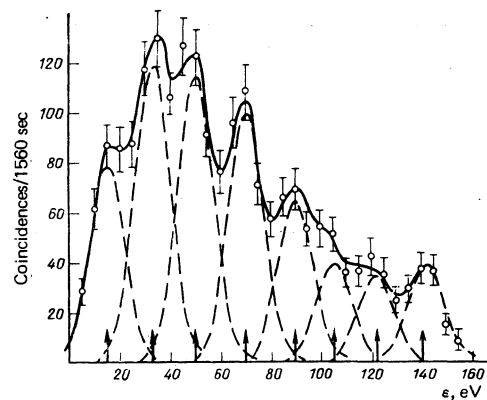


FIG. 1. Energy dependence of the coincidence count at $\vartheta = 45^\circ$; points—experiment, solid lines—sum of the dashed Gaussians.

We do not cite here the absolute binding energies of the observed state. The null point of the energy scale was chosen to be the position of the maximum of the peak on the extreme left, corresponding to knockout of electrons with minimum binding energy, i.e., the position of the maximum of the state density in the conduction band of aluminum.

The obtained spectra were reduced graphically. The statistical character and the smallness of the cross section of the observed processes, when the primary electron beam current must be kept low to prevent damage to the target, lead to definite experimental errors. This makes the reduction of the spectrum an incorrectly posed problem that has no unambiguous solution. However, a comparison of the spectra obtained by us with the results of experiments on aluminum and its oxide, wherein measurements were made of the photoelectron spectra²⁰ and of the characteristic electron energy losses,²¹ points to a number reference points. These are the maximum of the state density in the conduction band of aluminum with $\varepsilon = 0$, the $2s$ level of the oxygen atom with $\varepsilon \approx 20$ eV, and the $2p$ and $2s$ levels of aluminum with respective energies $\varepsilon \approx 75$ and 125 eV. In addition, the fact that the locations of the observed peaks recurred in measurements at different angles ϑ serves as additional evidence of the likelihood of our reduction.

Since the coincidence spectrum revealed not a single state far enough from its neighbors to permit its use for calibration of the setup, and since we were unable to simulate the $(e, 2e)$ process, the instrumental function for the measurements in the coincidence regime was determined from measurements of the spectrum of the primary electrons in one registration channel. It was found that the instrumental functions of both analyzers are well described by a Gaussian distribution with a variance $\sigma = 5$ eV. We have therefore assumed $\sigma = 7$ eV in the coincidence measurements. Since it can be assumed that the proper widths of all the observed states are much smaller than the instrumental width, the experimental results were interpreted by comparing them with the aid of a sum of Gaussian curves of the form $[A_i/(2\pi\sigma^2)]^{1/2} \times \exp[-(E - E_i)^2/2\sigma^2]$ with $\sigma = 7$ eV, where E_i is the position of the i th maximum and A_i is its amplitude. The solid line in Fig. 1 is the sum of the Gaussian curves (dashed) whose maxima are marked by the arrows.

"Shoot-through" measurements have shown that at $E_0 = 5$ keV and $\vartheta = 0^\circ$ the films used by us cause an insignificant broadening of the electron energy spectrum (the half-width of the spectrum for electron passing through aluminum films ~ 180 Å thick turned out to be ~ 2 eV larger than the instrumental half-width), and also that the intensity of the plasmon losses was $\sim 1/30$ of the intensity of the beam electrons, which passed through the film without energy loss. The results of these experiments are shown in Fig. 2. The fact that we have not observed in practice any excitation of a volume plasmon with $\hbar\omega_{p1} = 15.8$ eV in the aluminum is attributed to the small thickness of the target. It is known¹⁹ that for electrons with $E_0 = 10$ keV the mean free path for plasmon production in aluminum is ~ 260 Å.

The values obtained for the binding energies of the

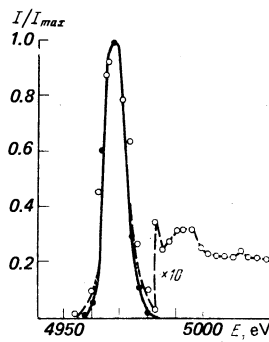


FIG. 2. Energy distribution of the electrons: dark circles—primary beam; light circles—after passing through a film ~ 180 Å thick at $\vartheta = 0^\circ$.

knocked-out electrons, reckoned from a level corresponding approximately to the Fermi energy ($\varepsilon_F^{\text{Al}} = 11.3$ eV), and the measured momentum distributions for the observed states, represented by angular correlation functions plotted for each of them, as well as a comparison with investigations of aluminum and oxide targets by methods of photoelectron spectroscopy and of the characteristic energy losses of the electrons,^{20, 21} have made it possible to identify the majority of the observed peak. The origin of the peaks with $\varepsilon = 45$ and 90 eV is still not clear; the first of them has a momentum distribution typical of p electrons, while the second corresponds possibly to a multiple plasmon satellite. We note that the peaks with $\varepsilon = 45$, 90 , and 105 eV were less distinct in the spectra than the remaining peaks, so that the results obtained for these states must be further refined.

The counting rate of the coincidences of the final electrons in the $(e, 2e)$ reaction is determined by the differential cross section

$$I_{\text{coinc}} = nI_0 \frac{d^4\sigma}{d\Omega_1 d\Omega_2 dE_1 dE_2} \Delta\Omega_1 \Delta\Omega_2 \Delta E_1 \Delta E_2 \delta(E_0 - E_1 - E_2 - \varepsilon_i), \quad (14)$$

where n is the density of the target particles, I_0 is the current of the primary electrons to the target, $\Delta\Omega_{1,2}$ and $\Delta E_{1,2}$ are the angular and energy resolutions of the registration channels. The dependence of I_{coinc} on the angle ϑ between the paths of the final electrons when a target electron with fixed binding energy ε_i is knocked out, in other words the angular dependence of the intensity of each maximum in the coincidence spectrum, is a function of the angular correlations, which in turn reflects the dependence of the differential cross section of the reaction $(e, 2e)$ on the target-electron momentum q prior to the interaction, which is connected with ϑ by relation (13). The angular-correlation function $I(q)$ was constructed by calculating the areas of the corresponding Gaussians, which are the results of the reduction of the spectra obtained at different values of ϑ . The experimental results were compared with the dependence of the differential cross section $d^4\sigma/d\Omega_1 d\Omega_2 dE_1 dE_2$ of the $(e, 2e)$ reaction on q in accord with formulas (7) and (19).

Figure 3 shows the experimental results (dark circles) as well as the theoretical distributions (dashed) obtained in the impulse approximation. All the curves are normalized to their maximum value. For convenience in the comparison, the theoretical curves take into account the finite angular resolution of the installation, which is due to the corresponding uncertainty in the value of q .

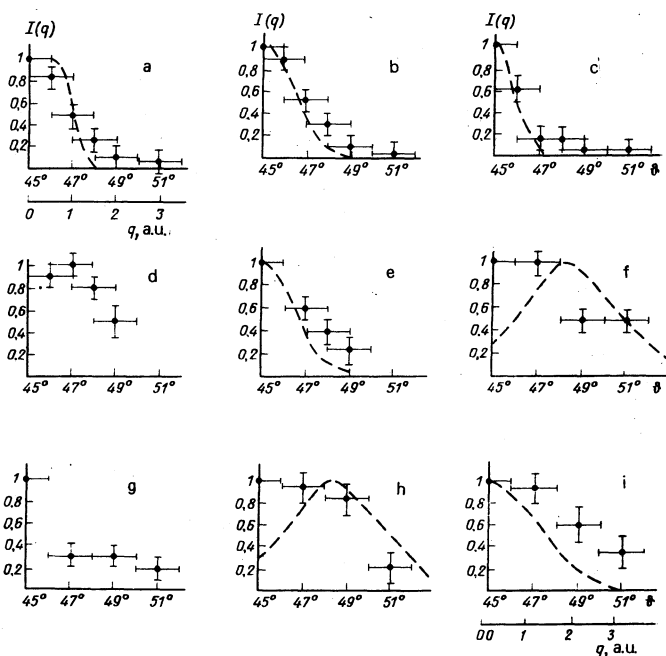


FIG. 3. Angular-correlation function (dark circles) for the following energy groups: a) "free" electrons; b) $\epsilon = 19$ eV; c) 32 eV, d) 43 eV; e) 55 eV; f) 75 eV; g) 90 eV; h) 105 eV; i) 125 eV; dashed lines—theoretical dependence of the differential cross section of the reaction ($e, 2e$) on q .

As seen from (7), in the case when electrons are knocked out of the conduction band the angular correlations correspond to a momentum distribution in the form of a step of width k_F (ideal Fermi gas). Figure 3a shows the results obtained for this case (some contribution is made to the experimental results also by electrons from the valence band of the aluminum oxide).

In accord with formula (10), when a deep hole is produced either in pure form or in the presence of a collective response of the conduction electrons (plasmon satellites) the angular-correlation function described the momentum distribution of the knocked-out electron. Figure 3b shows the angular-correlation function for the case of knockout of 2s electrons from an oxygen atom contained in the aluminum oxide ($\epsilon = 20$ eV). The agreement with the theory, as seen from the figure, is on the whole satisfactory, but the experimentally obtained distribution is somewhat broader than the theoretical one obtained with the aid of Hartree-Fock wave functions for 2s electrons of an isolated oxygen atom. We note that similar calculations for 1s electrons of the oxygen atom ($\epsilon = 530$ eV) gave good agreement with the ($e, 2e$) experiments performed by us previously, with practically the same angular resolution, on collodion films.¹⁴ The momentum distributions for the case when 2p and 2s electrons of Al are knocked out ($\epsilon \approx 75$ and 125 eV), shown in Figs. 3f and 3i, also differ somewhat from the calculated ones. The filling-up of the minimum at small q for the 2p states can apparently be attributed to distorted-wave effects, which become sizable when a deep hole is produced and manifest themselves most noticeably precisely for p states.²²

Figure 3e shows the results for the peak with $\epsilon \approx 55$ eV, which we interpret as a plasmon satellite of a 2s

hole in the oxygen atom in Al_2O_3 . The theoretical curve corresponds to the momentum distribution of the 2s electrons of an isolated oxygen atom (just as in Fig. 3b), since the plasmon momenta are close to zero. This state together with the states $\epsilon \approx 20$ and 32 eV, as seen from Fig. 1, is most strongly pronounced.

The angular correlations for the energy group with $\epsilon \approx 105$ eV are shown in Fig. 3h. The distribution obtained is similar to that observed for the 2p electrons of Al (Fig. 3e), and this state is separated from the 2p level of Al by ~ 30 eV on the energy scale. It can therefore be concluded that this group corresponds to excitation of a plasmon satellite in Al_2O_3 .

The momentum distribution shown in Fig. 3c and corresponding to the state with $\epsilon \approx 32$ eV turned out to be half as wide as the distribution obtained for the individual act of electron knockout from the conduction band. This gives us ground for interpreting this state as the Lundqvist plasmaron.⁶ The energy position of this peak agrees well with the value $\epsilon_{p1r} = 2\hbar\omega_{p1} = 31.6$ eV reckoned from the Fermi level, which determines the second ϵ singularity of the function $A(q, \epsilon)$ in formula (7). The theoretical momentum distribution for this state was plotted on the basis of Lundqvist's calculations⁶ for the average distances $r_s \approx 2$ between the electrons in the electron gas, which is a characteristic of aluminum. The agreement with the theory is satisfactory.

The plasmaron was not observed prior to the use of the ($e, 2e$) method, despite of attempts to separate it in experiments on photoelectron spectroscopy using soft x rays and synchrotron radiation.^{23, 24} The reason is that the plasmaron practically coincides in energy with a multiple plasmon excitation. Only an investigation of the momentum distribution for a selected energy group

makes it possible to distinguish most reliably between a plasmaron and ordinary plasmon production "in flight" by fast electrons passing through an electron gas. In fact, the momentum distributions of ordinary plasmon satellites would duplicate the distribution for a Fermi gas, i.e., Fig. 3a.

The observation of the Lundqvist plasmaron is of interest because the theory of this question⁶ was quite roughly simplified (first-order perturbation theory), and the validity of the results was not obvious. To pass final judgement, we plan to improve the resolution by a factor 1.5–2, and this will make it possible also to assess the intensities of the peaks.

In conclusion the authors are sincerely grateful to V. G. Levin and A. V. Pavlichenkov for valuable advice and help, and to S. V. Gubin for help with the experiments.

¹Yu. F. Smirnov and V. G. Neudachin, *Pis'ma Zh. Eksp. Teor. Fiz.* **3**, 298 (1966) [*JETP Lett.* **3**, 192 (1966)]; V. G. Neudachin, G. A. Novoskol'tseva, and Yu. F. Smirnov, *Zh. Eksp. Teor. Fiz.* **55**, 1039 (1968) [*Sov. Phys. JETP* **28**, 540 (1969)]; A. E. Glassgold and G. Ialongo, *Phys. Rev.* **175**, 151 (1968); V. G. Levin, *Phys. Lett. A* **39**, 125 (1972); J. B. Furness and I. E. McCarthy, *J. Phys. B* **6**, 2280 (1973); **7**, 541 (1974); V. G. Levin, V. G. Neudatshin, A. V. Pavlitchenkov, and Yu. F. Smirnov, *J. Chem. Phys.* **63**, 1541 (1975); I. E. McCarthy, *J. Phys. B* **8**, 2133 (1975); V. G. Levin and A. V. Pavlitchenkov, *Phys. Lett. A* **58**, 451 (1976).

²V. G. Neudatchin and F. A. Zhivopistsev, *Phys. Rev. Lett.* **32**, 995 (1974).

³N. A. Krasil'nikova and N. M. Presiantseva, *Pis'ma Zh. Tekh. Fiz.* **4**, 868 (1978) [*Sov. Tech. Phys. Lett.* **4**, 351 (1978)].

⁴V. L. Bonch-Bruevich and S. V. Tyablikov, *Metod funktsii Grina v statisticheskoi mekhanike* (The Green's Function Method in Statistical Mechanics), Fizmatgiz, 1961; A. A. Abrikosov, L. P. Gor'kov, and I. E. Dzyaloshinskii, *Metody kvantovoi teorii polya v statisticheskoi fizike* (Quantum Field Theoretical Methods in Statistical Physics), Fizmatgiz, 1962 [Pergamon, 1965].

⁵R. N. West, *Adv. Phys.* **22**, 263 (1973); I. A. Dekhtiar, *Phys. Rep.* **9**, 243 (1974).

⁶S. I. Lundqvist, *Phys. Kondens. Mater* **6**, 193, 206 (1967); **7**, 117 (1968); **9**, 231, 236 (1969); L. Hedin, B. I. Lundqvist, and S. Lundqvist, *J. Res. Nat. Bur. Stand. A* **74**, 417 (1970).

⁷W. Fritsch, R. Lipperheids, and U. Wille, *Nucl. Phys. A* **198**, 515 (1972); *Phys. Lett. B* **45**, 103 (1973).

⁸G. D. Mahan, *Phys. Rev.* **163**, 612 (1967); P. Nozieres and S. I. Dominicis, *Phys. Rev.* **178**, 1097 (1969); P. Nozieres and E. Abrahams, *Phys. Rev. B* **10**, 3099 (1974); G. K. Worthheim and S. Hüfner, *Phys. Rev. Lett.* **35**, 53 (1975); J. D. Dow, *Commun. Solid State Phys.* **6**, 71 (1975).

⁹D. C. Langreth, *Phys. Rev. B* **1**, 471 (1970); T. T. Chang and D. C. Langreth, *Phys. Rev. B* **5**, 3512 (1972).

¹⁰V. G. Levin, V. G. Neudatchin, and Yu. F. Smirnov, *Phys. Status Solidi B* **49**, 489 (1971); L. Vriens, *Phys. Rev. B* **6**, 3088 (1971).

¹¹J. O. Porteus and W. N. Faith, *Phys. Rev. B* **12**, 2097 (1975).

¹²M. Sunjic and D. Sokcevic, *Solid State Commun.* **18**, 373 (1976).

¹³C. S. Ting, *J. Phys. F* **1**, 945 (1971); *Phys. Rev. B* **6**, 4185 (1972).

¹⁴N. A. Krasil'nikova, V. G. Levin, and N. M. Persiantseva, *Zh. Eksp. Teor. Fiz.* **69**, 1562 (1975) [*Sov. Phys. JETP* **42**, 796 (1975)].

¹⁵R. Camilloni, A. Giardini-Guidoni, R. Tiribelli, and G. Stefani, *Phys. Rev. Lett.* **29**, 618 (1972).

¹⁶Abdallah Ibrahim Mohamed, *Dissertation, Nucl. Physics Inst. of the Moscow State Univ.*, 1976.

¹⁷L. I. Andreeva, V. A. Belokon', T. M. Malinina, R. R. Odintsova, and A. I. Yuzhin, *Prib. Tekh. Eksp. No. 2*, 228 (1975).

¹⁸T. Farrell and R. D. Naybour, *Nature (London) Phys. Sci.* **244**, 14 (1973).

¹⁹G. V. Jewell, transl. in: *Kharakteristicheskie poteri énergii élektronov v tverdykh telakh* (Characteristic Energy Losses of Electrons in Solids), ed. by A. R. Shul'man, IIL, 1959, p. 84.

²⁰A. Balzarotti and A. Bianconi, *Phys. Status Solidi B* **76**, 689 (1976).

²¹C. Benndorf, G. Keller, H. Seidel, and T. Thieme, *Surf. Sci.* **67**, 589 (1977).

²²I. E. McCarthy and E. Weigold, *Phys. Rev. C* **27**, 275 (1976).

²³W. J. Pardee, G. D. Mahan, D. E. Eastman, R. A. Pollak, L. Ley, F. R. McFeely, S. P. Kovalczyk, and D. A. Shirley, *Phys. Rev. B* **11**, 3614 (1975).

²⁴S. A. Flodstrom, R. Z. Bachrach, R. S. Bauer, J. C. McMennamin, and S. M. B. Hangstrom, *J. Vac. Sci. Technol.* **14**, 303 (1977).

Translated by J. G. Adashko